Journal of Sound and Vibration (1998) **216**(4), 601–621
Article No. sv981716

NON-LINEAR VIBRATION OF A MULTILAYER SANDWICH BEAM WITH VISCOELASTIC LAYERS

H.-H. Lee

Department of Marine Environment, *National Sun Yat-sen University*, *Kaohsiung*, *Taiwan*

(*Received* 13 *September* 1996, *and in final form* 26 *March* 1998)

A finite element formulation combined with a new material model has been developed for the traditional multilayer beam incorporating viscoelastic material having non-linear behavior. The viscoelastic material was confined between the stiff layers and worked as a damping layer. A non-linear dynamic analysis in the time domain was carried out for the multilayer beam subjected to dynamic loadings. In the analysis the boundary conditions for the beam are either simple or clamped and the exerted loadings include transient impulse loading, harmonic excitation and a random type process. The non-linear responses in the time domain for the multilayer sandwich beam containing the viscoelastic material were compared to one without the viscoelastic material. The time domain dynamic behavior for the multilayer beam with variant boundary conditions, dimensions and loading types is also discussed.

1. INTRODUCTION

When structures are subjected to dynamic loadings tremendous amounts of energy are input into the structural system usually. In order to mitigate the vibration and so avoid serious damage, viscoelastic material, which has substantial energy absorption ability, can be incorporated in the structural system. An example is the sandwich beam with viscoelastic core between the stiff layers, which was first introduced by Swallow [1] as early as 1939. Since then a number of investigations on the design formulation for the three layer damped sandwich beam have been carried out by many researchers. Kerwin [2] suggested a complete and simplified formula for the estimation of loss factor dependent on the wavelength of bending waves, the thickness of the constraining layer, and elastic moduli of the plate, damping layer and constraining layer. Ungar and Kerwin [3] then correlated the loss factors to energy concepts. Di Taranto [4] derived a sixth order complex homogeneous differential equation for a free vibrating finite-length sandwich beam. Di Taranto and Blasingame [5, 6] continued Kerwin's work and published the dependency between the damping (in terms of loss factor) and the frequency for selected laminated beams. Mead and Markus [7] continued the work and developed a sixth order differential equation in terms of transverse displacement

0022–460X/98/390601 + 21 $30.00/0

for the forced vibration of the sandwich beam under specific "damped normal loadings". Mead [8] later made a comparison of these equations for the flexural vibration and the loss factors. In this research the analytical formulations for the sandwich beam were accurate for the elastic system with linear damping in the fairly high frequency range.

Lately, due to the frequent occurrence of major earthquakes which have caused extensive damage to buildings, bridges and other civil structures, a viscoelastic material suitable for low frequency applications in civil building systems, has been developed. As presented in the results of experimental testing for this viscoelastic material [9–12], non-linear behavior was observed in the stress–strain relationship, particularly during the higher frequency loading test (still lower than about 10 Hz). As was shown by the results, the stress was not only dependent on the loading frequency but the strain ratio. During the large strain cycling, temporary lowering of the shear modulus because of material softening induced by the heat built-up was found. This effect is reversed after the heat is dissipated and the temperature returns to its original ambient value. Therefore, it is not suitable to use traditional complex models to describe this non-linear behavior for the viscoelastic material. To overcome this problem an analytical material model for this viscoelastic damper, which can accurately describe the mechanical behavior, was developed by Lee and Tsai [13, 14].

By using this model, evaluations have been made for some typical structural systems which were incorporated with the damping devices [15–18] and good results in dynamic performances were obtained. It is the purpose of this study to combine this non-linear material model with the multilayer beam system containing the viscoelastic material, and to study further its non-linear dynamic behavior in the time domain when subjected to a variety of loadings and boundary conditions.

2. THE ANALYTICAL MODEL OF THE VISCOELASTIC MATERIAL

In order to predict adequately the behavior of a structural material subjected to dynamic loading, an analytical model must be capable of representing the typical material characteristics and adequately describing the dynamic behavior. By utilizing the molecular theory and Bagley and Torvic's [19, 20] fractional derivative viscoelastic model, a non-linear analytic model has been derived and modified using the available experimental results. The constitutional formula, having a fractional derivative form, is presented as

$$\tau(t) = G'\gamma(t) + G''D^{\alpha}(\gamma(t)), \qquad 0 < \alpha < 1, \tag{1}$$

where τ and γ are the stress and strain of the material, G' and G'' represent the shear modulus corresponding to the storage and the loss energy respectively. According to the model derived by Lee and Tsai [13, 14], the modulus degradation and the thermal effect are taken into consideration. Considering a temperature

difference $\Delta T = T - T_0$ from the referred temperature T_0, the material elastic moduli are given by

$$G' = G'' = A_0 \exp[\beta_1 \Delta T + \beta_2 |\Delta T| + \beta_3 \operatorname{sgn}(\Delta T)]\left[1 + B_0 \exp\left(-\beta \int \tau \, \mathrm{d}\gamma\right)\right], \tag{2}$$

where B_0 and β are coefficients to account for the energy absorption ability of the material; A_0 is the coefficient corresponding to the original modulus of the material, and β_1–β_3 are coefficients corresponding to the thermal effect. All of these unknown coefficients are material-dependent and determined by the experimental data. The fractional derivative is accordingly presented as

$$D^{\alpha}(\gamma(t)) = \frac{1}{\Gamma(1-\alpha)} \frac{\mathrm{d}}{\mathrm{d}t} \int_0^t \frac{\gamma(t)}{(t-\lambda)^{\alpha}} \, \mathrm{d}\lambda, \qquad 0 < \alpha < 1, \tag{3}$$

where $\Gamma(1-\alpha)$ is the gamma function.

To apply the fractional derivative model to the time-domain analysis, a numerical scheme using the finite element method is proposed. For the linear variation of the strain between two time steps, $(n-1)\Delta t$ and $n\Delta t$, a constitutive law for the viscoelastic damper at time step $n\Delta t$ can subsequently be written as

$$\tau(n\Delta t) = \left[G' + \frac{G''(\Delta t)^{-\alpha}}{(1-\alpha)\Gamma(1-\alpha)}\right]\gamma(n\Delta t) + \tau_p(n\Delta t). \tag{4}$$

The previous time effect of the strain, $\tau_p(n\Delta t)$, is defined as

$$\tau_p(n\Delta t) = \frac{G''\Delta t^{-\alpha}}{(1-\alpha)\Gamma(1-\alpha)}\left(W_0^n \gamma(0) + \sum_{i=1}^{n-1} W_i^n \gamma(i\Delta t)\right), \tag{5}$$

where W_0^n and W_i^n are functions corresponding to time step n:

$$W_0^n = (n-1)^{1-\alpha} + (-n+1-\alpha)n^{-\alpha}$$

and

$$W_i^n = -2(n-i)^{1-\alpha} + (n-i+1)^{1-\alpha} + (n-i-1)^{1-\alpha}.$$

A typical force–displacement relationship representing the mechanical behavior of the viscoelastic damper is shown in Figure 1, where (a) represents the experimental data and (b) shows the results of analytical simulation from the model. It is observed that a great amount of energy can be absorbed during each cycle of hysteretic motion of the material and this mechanical behavior is adequately simulated by the analytical model.

3. GENERAL THEORY OF MULTILAYER SANDWICH BEAMS WITH VISCOELASTIC LAYER

A five-layer sandwich beam, incorporating viscoelastic damping material as shown in Figure 2, where the top, middle and the bottom layers were stiff materials separated by layers of viscoelastic material. Following previous theories developed for the multilayer sandwich beam [21–23], a multilayer sandwich beam with viscoelastic material in the shear layer has been derived here by using the analytical constitutive model for the viscoelastic material. For the ith stiff layer, the relationship between bending moment M_i and vertical displacement w is given by

$$M_i = -E_i I_i \, \mathrm{d}^2 w / \mathrm{d}x^2, \qquad i = 1\text{–}3, \tag{6}$$

and the relationship between axial force N_i and axial displacement u_i is given by

$$N_i = E_i b_i t_i \, \mathrm{d}u_i / \mathrm{d}x, \qquad i = 1\text{–}3, \tag{7}$$

where E_i and I_i are the elastic modulus and the moment of inertia of the ith stiff layer respectively.

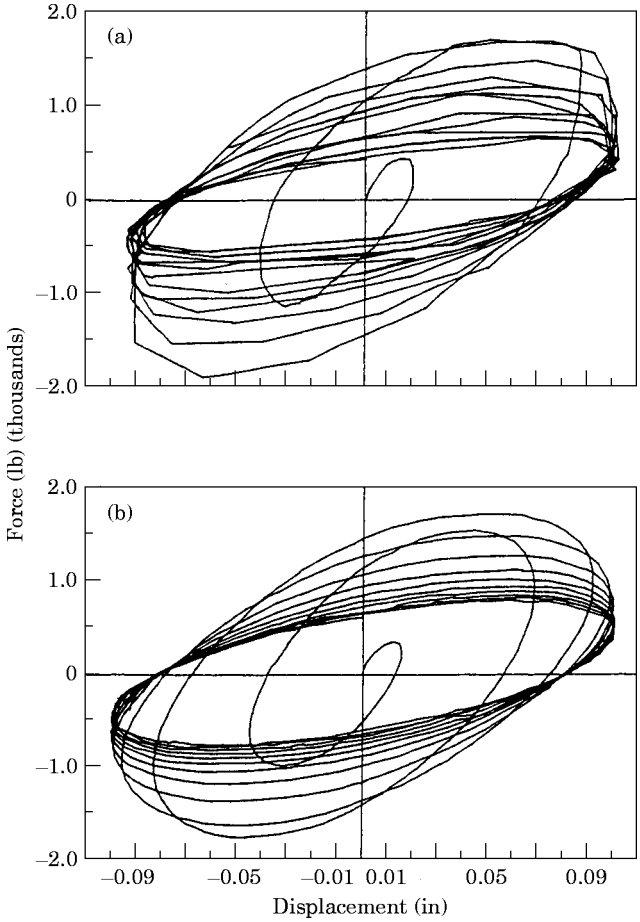

Figure 1. Typical force–displacement relationship for the damping material: (a) experimental data; (b) analytical results (after Lee and Tsai, 1994).

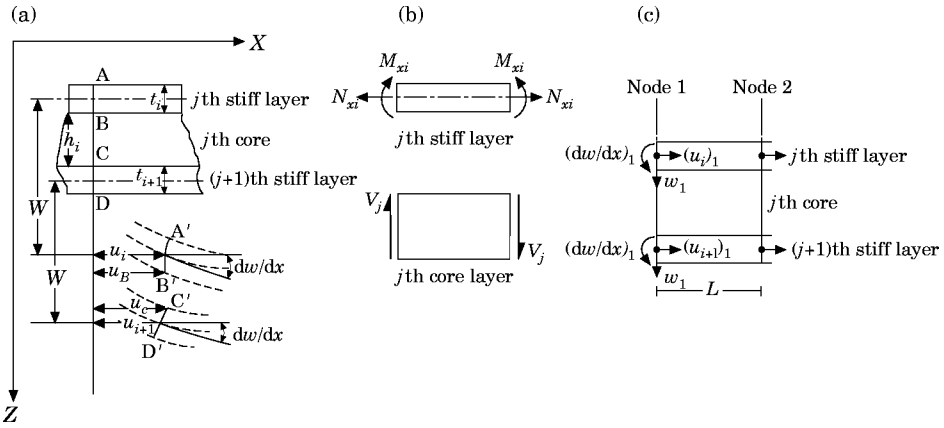

Figure 2. Five layer sandwich beam: (a) indication of deformation; (b) general forces; (c) nodal displacement in the typical element (redrawn after Khatua and Cheung, 1973).

The shear strain in the jth viscoelastic layer is given by

$$\gamma_j = (u_{i+1} - u_i)/h_j + (C_j/h_j)\,\mathrm{d}w/\mathrm{d}x, \qquad j = 1, 2, \tag{8}$$

where

$$C_j = h_j + \tfrac{1}{2}(t_{i+1} + t_i). \tag{9}$$

Correspondingly if the viscoelastic material was applied in these shear layers and the non-linear material behavior in the time domain was taken into account, in the discrete time domain for time step $n\Delta t$ the shear force in the jth shear layer can be written in terms of the shear strain, time increment and the non-linear shear modulus as

$$V_j(n\Delta t) = (G_j' + G_j''(\Delta t)^{-\alpha}/(1-\alpha)\Gamma(1-\alpha))b_j h_j \gamma_j(\Delta t) + V_{jp}(\Delta t), \quad j = 1, 2, \tag{10}$$

where V_{jp} represents a previous non-linear effect of the material. Now through the substitution of the shear strain (equation (8)) into equation (10) and after the combination with equations (6) and (7), again at time step $n\Delta t$ in the discrete time domain the relationship between the nodal force vector and the strain vector is given in a matrix form by

$$\sigma(\mathbf{n\Delta t}) = \mathbf{D}\epsilon(\mathbf{n\Delta t}) + \sigma_p(\mathbf{n\Delta t}), \tag{11}$$

where the nodal force vector is

$$\sigma(\mathbf{n\Delta t}) = \begin{pmatrix} M_1(n\Delta t) \\ N_1(n\Delta t) \\ V_1(n\Delta t) \\ M_2(n\Delta t) \\ N_2(n\Delta t) \\ V_2(n\Delta t) \\ M_3(n\Delta t) \\ N_3(n\Delta t) \end{pmatrix} \tag{12}$$

the strain vector is represented as

$$\epsilon(\mathbf{n\Delta t}) = \begin{Bmatrix} -\mathrm{d}w^2(n\Delta t)/\mathrm{d}x^2 \\ \mathrm{d}u_1(n\Delta t)/\mathrm{d}x \\ \gamma_1(n\Delta t) \\ -\mathrm{d}w^2(n\Delta t)/\mathrm{d}x^2 \\ \mathrm{d}u_2(n\Delta t)/\mathrm{d}x \\ \gamma_2(n\Delta t) \\ -\mathrm{d}w^2(n\Delta t)/\mathrm{d}x^2 \\ \mathrm{d}u_3(n\Delta t)/\mathrm{d}x \end{Bmatrix}, \tag{13}$$

and $\mathbf{D}$ is a diagonal matrix with elements

$$D_{jj} = \begin{Bmatrix} D_{11} = E_1 I_1 \\ D_{22} = E_1 b_1 t_1 \\ D_{33} = (G_1' + G_1'' \Delta t^{-\alpha}/\Gamma(2-\alpha)) b_1 h_1 \\ D_{44} = E_2 I_2 \\ D_{55} = E_2 b_2 t_2 \\ D_{66} = (G_2' + G_2'' \Delta t^{-\alpha}/\Gamma(2-\alpha)) b_2 h_2 \\ D_{77} = E_3 I_3 \\ D_{88} = E_3 b_3 t_3 \end{Bmatrix}. \tag{14}$$

The force vector corresponding to the previous effect of the shear induced by the viscoelastic material is given by

$$\sigma_p(\mathbf{n\Delta t}) = (0, 0, V_{1p}(n\Delta t), 0, 0, V_{2p}(n\Delta t), 0, 0)^{\mathrm{T}}, \tag{15}$$

where through equation (5)

$$V_{kp}(n\Delta t) = \frac{h_k b_k G_k'' \Delta t^{-\alpha}}{(1-\alpha)\Gamma(1-\alpha)} \left(W_0^n \gamma_k(0) + \sum_{i=1}^{n-1} W_i^n \gamma_k(i\Delta t) \right), \qquad k = 1, 2. \tag{16}$$

4. FINITE ELEMENT FORMULATION OF A DAMPED MULTILAYER SANDWICH BEAM

A typical element for the beam incorporated with viscoelastic material is derived here. The displacements for a typical element at nodal points 1 and 2 are $\mathbf{X_1(t)}$ and $\mathbf{X_2(t)}$ respectively:

$$\mathbf{X_1(t)} = \begin{Bmatrix} a_1(t) \\ a_2(t) \\ a_3(t) \\ a_4(t) \\ a_5(t) \end{Bmatrix}, \qquad \mathbf{X_2(t)} = \begin{Bmatrix} a_6(t) \\ a_7(t) \\ a_8(t) \\ a_9(t) \\ a_{10}(t) \end{Bmatrix}, \tag{17, 18}$$

where $a_1(t)$ and $a_6(t)$ are transverse displacements and $a_2(t)$ and $a_7(t)$ are rotations at node 1 and node 2 respectively; $a_3(t)$–$a_5(t)$ and $a_8(t)$–$a_{10}(t)$ are axial displacements corresponding to three stiff layers at node 1 and node 2 respectively as shown in Figure 2(c).

Now the strains are further related to the displacements as

$$\epsilon(\mathbf{t}) = \mathbf{LU(t)}, \tag{19}$$

where $\mathbf{L}$ is an operational matrix and $\mathbf{U}$ is the displacement field vector. The displacement field vector is related to the nodal displacements by

$$\mathbf{U(t)} = \mathbf{NX(t)}, \tag{20}$$

where

$$\mathbf{X(t)} = \begin{Bmatrix} \mathbf{X_1(t)} \\ \mathbf{X_2(t)} \end{Bmatrix}, \qquad \mathbf{N} = [\mathbf{N_1}, \mathbf{N_2}], \tag{21, 22}$$

with

$$\mathbf{N_1} = \begin{bmatrix} 1 - 3(x^2/L^2) + 2(x^3/L^3) & x - 2(x^2/L) + x^3/L^2 & 0 & 0 & 0 \\ 0 & 0 & 1 - x/L & 0 & 0 \\ 0 & 0 & 0 & 1 - x/L & 0 \\ 0 & 0 & 0 & 0 & 1 - x/L \end{bmatrix}, \tag{23}$$

and

$$\mathbf{N_2} = \begin{bmatrix} 3(x^2/L^2) - 2(x^3/L^3) & -x^2/L + x^3/L^2 & 0 & 0 & 0 \\ 0 & 0 & x/L & 0 & 0 \\ 0 & 0 & 0 & x/L & 0 \\ 0 & 0 & 0 & 0 & x/L \end{bmatrix}. \tag{24}$$

Therefore, the strains in terms of the nodal displacements at time step $n\Delta t$ in the discrete time domain become

$$\epsilon(\mathbf{n}\Delta\mathbf{t}) = \mathbf{LU}(\mathbf{n}\Delta\mathbf{t}) = \mathbf{LNX}(\mathbf{n}\Delta\mathbf{t}) = \mathbf{BX}(\mathbf{n}\Delta\mathbf{t}). \tag{25}$$

Substitution of equations (15) and (25) into equation (11) and using the virtual work principle leads to the stiffness matrix and the previous time effect vector for the finite element formulation as

$$\mathbf{K^e} = \int_{\mathbf{L^e}} \mathbf{B^T D B}\, \mathrm{d}x, \qquad \mathbf{F_p^e}(\mathbf{n}\Delta\mathbf{t}) = \int_{\mathbf{L^e}} \mathbf{B^T}\sigma_p(\mathbf{n}\Delta\mathbf{t})\, \mathbf{dx} \tag{26, 27}$$

In the discrete time domain at time step $n\Delta t$ and taking into account the previous time effect for the viscoelastic material in the shear layers, the dynamic equation of motion for the beam element with mass $\mathbf{M}^e$, damping coefficient $\mathbf{C}^e$, and stiffness $\mathbf{K}^e$, subjected to loading $\mathbf{P}^e(\mathbf{n\Delta t})$ can be written as

$$\mathbf{M}^e\ddot{\mathbf{X}}(\mathbf{n}\Delta\mathbf{t}) + \mathbf{C}^e\dot{\mathbf{X}}(\mathbf{n}\Delta\mathbf{t}) + \mathbf{K}^e\mathbf{X}(\mathbf{n}\Delta\mathbf{t}) = \mathbf{P}^e(\mathbf{n}\Delta\mathbf{t}) - \mathbf{F}_p^e(\mathbf{n}\Delta\mathbf{t}), \tag{28}$$

where the mass matrix is

$$\mathbf{M}^e = \int_{\mathbf{L}^e} \mathbf{N}^T\mathbf{m}\mathbf{N}\,\mathbf{dx}, \tag{29}$$

obtained through the diagonal matrix $\mathbf{m}$ represented by the material densities such as ρ_s, density of stiff layer and ρ_c, density of core layer of which the elements are

$$m_{jj} = \begin{cases} m_{11} = \left(\sum_{i=1}^{3} \rho_{si}t_i + \sum_{i=1}^{2} \rho_{ci}h_i\right)b \\ m_{22} = (\rho_{s1}t_1 + \frac{1}{2}\rho_{c1}h_1)b \\ m_{33} = [\rho_{s2}t_2 + \frac{1}{2}(\rho_{c1}h_1 + \rho_{c2}h_2)]b \\ m_{44} = (\rho_{s3}t_3 + \frac{1}{2}\rho_{c2}h_2)b \end{cases}, \tag{30}$$

and the damping matrix $\mathbf{C}^e$ may be obtained through the linear combination of mass matrix and stiffness matrix or solely from the mass matrix as customary application due to the uncertainty of the system damping.

Having obtained the equations of motion and the forces exerted on the structural system, the analysis can be carried out by using step-by-step integration schemes for non-linear structural systems such as Newmark-β method [24], Wilson's method [25] etc.. In this study the Newmark method using an average acceleration operator was adopted due to its numerical stability advantage.

5. NUMERICAL RESULTS AND DISCUSSION

In the numerical analysis, a typical five-layer sandwich beam having viscoelastic layers between the stiff layers was modelled and analyzed in the time domain. The boundary conditions at both ends of the beam were assumed to be simply supported firstly and then clamped. For the simply supported condition, transverse constraint was applied to all layers at both supported ends while axial constraint was applied to the middle stiff layer at one end, and to the top and bottom stiff layers at the other end. For the clamped boundary condition the transverse and axial displacement and the rotation were assumed to be constrained at the ends. The loading was assumed to be concentrated and exerted on the middle point of the beam. The magnitude of the loading was arbitrarily chosen so that a small displacement was produced. The loading types adopted in the analysis include transient impulse loading, harmonic excitation and alternately applied random excitations.

The geometrical dimensions for the beam and each layer of the material were adopted from Khatua and Cheung's example [23] as: $b = 1{\cdot}00$ in, $h_1 = h_2 = 0{\cdot}40$ in, $t_1 = t_2 = t_3 = 0{\cdot}02$ in. The material properties, assumed to be constant, were: the elastic modulus $E_s = 10 \times 10^6$ psi for the stiff layers and the shear modulus $G_3 = 48$ psi for the core layers. The viscoelastic material used in the analysis has coefficients as following: $B_0 = 1$, $\alpha = 0{\cdot}75$, $\beta = 0{\cdot}001$, $\beta_1 = -0{\cdot}089$, $\beta_2 = 0{\cdot}0153$, and $\beta_3 = 0{\cdot}12$. In order that the original stiffness is compatible with that of the beam for which the non-linear viscoelastic behavior for the cores was ignored, the coefficient A_0 correlated to the shear modulus of the viscoelastic material is given to be $G_s/2$.

To be able to reflect the damping effect that has solely resulted from the viscoelastic material, the system damping was ignored in the analysis. The analysis was focused on the response of the displacement, velocity and acceleration induced by the input loading and the effect of response reduction when the viscoelastic damping layers were applied. The results were obtained by carrying out the calculation for the coupled MDOF non-linear system, and are plotted and presented in the figures. The analysis was categorized into six groups: five examples corresponded to five sets of loading that were applied to the multilayer sandwich beam with either clamped or simple boundary conditions at the supports, and one additional example corresponded to the dimensional effect when the thickness of the layers was varied. The first loading is a transient impulse loading. The second, the third and the fourth loadings are harmonic of which the frequency applied is either resonant with, or lower than or higher than the dominant frequency of the beam. The fifth loading is a broad band random process.

5.1. MULTILAYER SANDWICH BEAM SUBJECTED TO TRANSIENT IMPULSE

In this analysis an impulse loading was assumed to be suddenly exerted on the middle point of the multilayer sandwich beam, of which both ends were simply supported. The loading duration was assumed to be 0·01 s. Figures 3–5 show the comparison of the time domain response of the transverse displacement, velocity and acceleration for the middle node of the beam with respect to the beam in which the viscosity of the core layer was not taken into account. Figure 6 shows the comparison of the response for the rotation of the middle point, and Figure 7

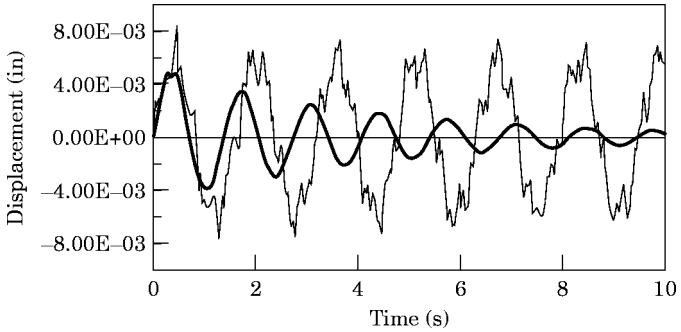

Figure 3. Comparison of the transverse displacement response (transient impulse loading, simply supported). Key: ——, no viscoelastic layer; ——, with viscoelastic layer.

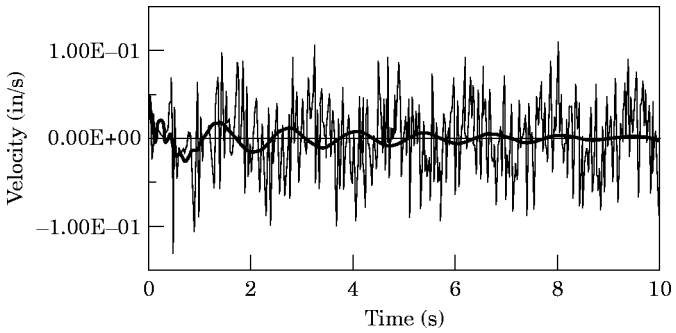

Figure 4. Comparison of the transverse velocity response (transient impulse loading, simply supported). Key as for Figure 3.

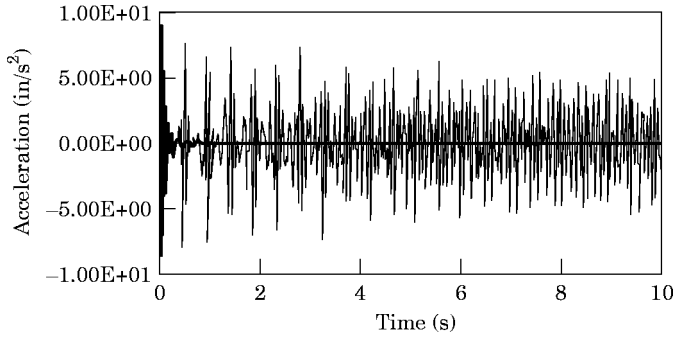

Figure 5. Comparison of the transverse acceleration response (transient impulse loading, simply supported). Key as for Figure 3.

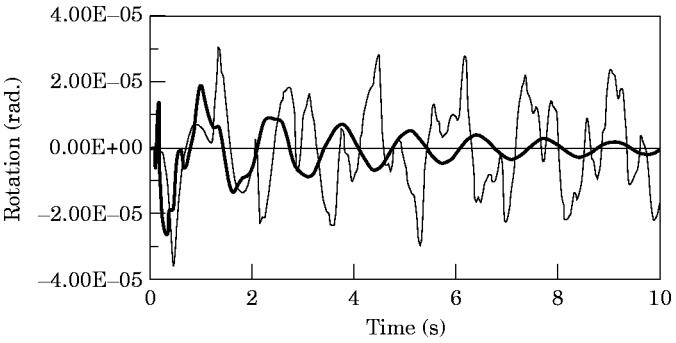

Figure 6. Comparison of the rotation response (transient impulse loading, simply supported). Key as for Figure 3.

shows the relative axial displacement comparison between the top and the middle stiff layer, where during the early loading stage the damped reaction was largely due to the release of the axial constraint at the ends but which became small subsequently. It is observed from the analytical results that the responses for each case decayed gradually due to the non-linear viscosity damping effect. According to the transverse displacement response the initial amplitude drop is about 43% compared to the beam with a similar stiffness but without viscosity. The damping factor estimated from the logarithmic decrement method is about 5·30% between the first and the second peak, and 4·20% between the second and the third peak.

5.2. MULTILAYER SANDWICH BEAM SUBJECTED TO RESONANT HARMONIC LOADING

In this analysis both of the multilayer sandwich beam with the simple support and the beam with clamped ends were analyzed when resonant harmonic loading was applied. For the simply supported beam the resonant frequency is 0·635 Hz while for the clamped beam the resonant frequency is 0·822 Hz. Figures 8 and 9 show the comparison of the response of the displacement and velocity respectively at the middle point for the simply supported beam, while Figures 10 and 11 show the same responses for the beam with clamped boundary conditions. A phase

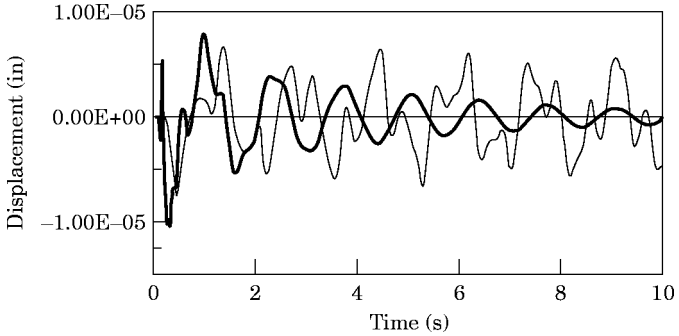

Figure 7. Comparison of the axial displacement response (transient impulse loading, simply supported). Key as for Figure 3.

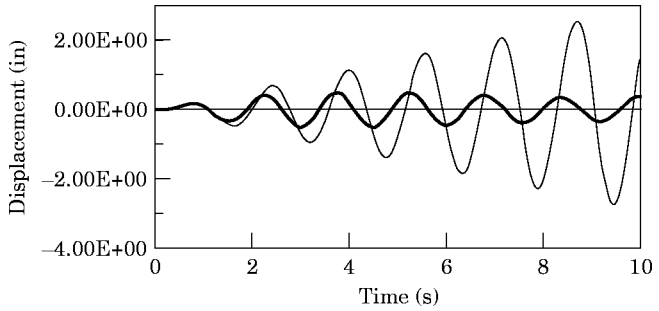

Figure 8. Comparison of the transverse displacement response (resonant harmonic loading, simply supported). Key as for Figure 3.

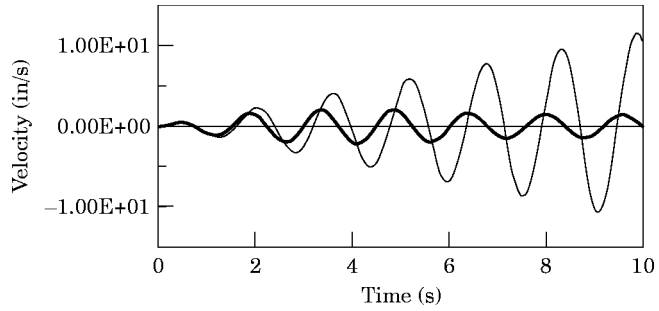

Figure 9. Comparison of the transverse velocity response (resonant harmonic loading, simply supported). Key as for Figure 3.

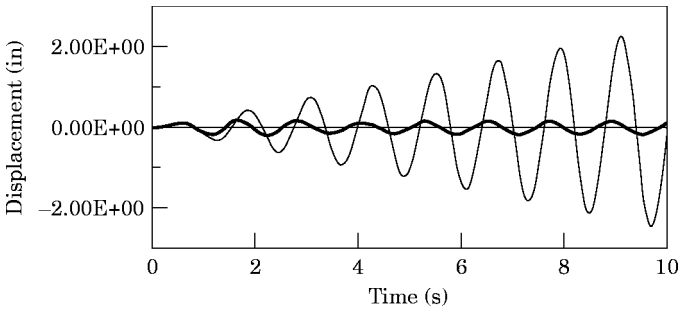

Figure 10. Comparison of the transverse displacement response (resonant harmonic loading, clamped boundary condition). Key as for Figure 3.

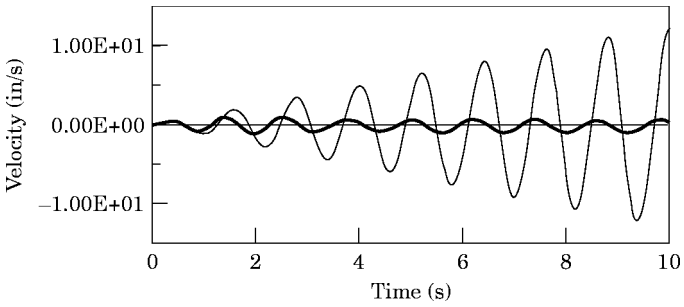

Figure 11. Comparison of the transverse velocity response (resonant harmonic loading, clamped boundary condition). Key as for Figure 3.

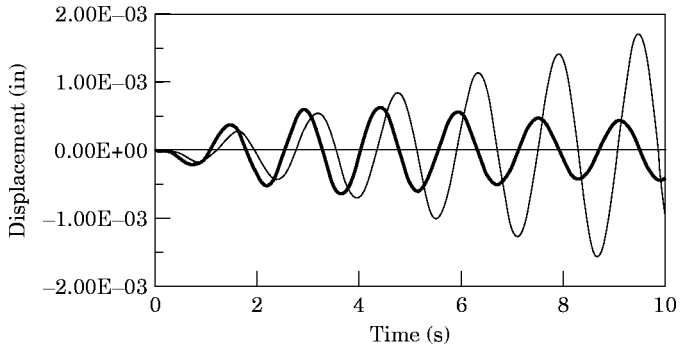

Figure 12. Comparison of the axial displacement response (resonant harmonic loading, simply supported). Key as for Figure 3.

difference between the displacement and the velocity response is shown. The response amplitudes were magnified when the viscosity of the material was ignored, whereas, as indicated by the heavier curves, the magnification was lessened by the viscoelastic damping effect. Figure 12 showed the comparison of the axial displacement response for the top stiff layer relative to the middle stiff layer for the simple beam system. It shows that during the early loading stage the damped reaction was relatively larger when compared to the one without damping effect, but it remained about the same while the reaction of the undamped beam escalates continually in the later loading stage.

5.3. MULTILAYER SANDWICH BEAM SUBJECTED TO LOW FREQUENCY HARMONIC LOADING

In this analysis a loading of 0·2 Hz frequency, which is relatively lower than the resonant frequency, was applied for both the simple beam and clamped beam system. Figures 13–15 show the comparison of the time domain response of the transverse displacement, velocity and acceleration for the middle point of the simple multilayer sandwich beam. Figures 16–18 show a comparison of the response of the transverse displacement, velocity and acceleration for the middle point of the clamped multilayer sandwich beam. Similarly to the resonant

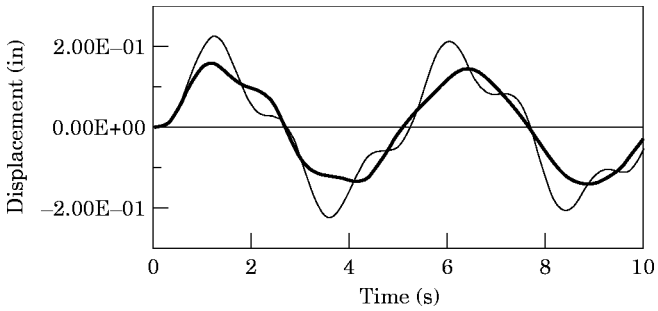

Figure 13. Comparison of the transverse displacement response (low frequency harmonic loading, simply supported). Key as for Figure 3.

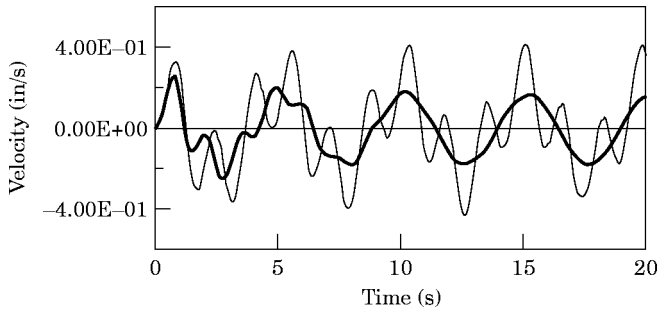

Figure 14. Comparison of the transverse velocity response (low frequency harmonic loading, simply supported). Key as for Figure 3.

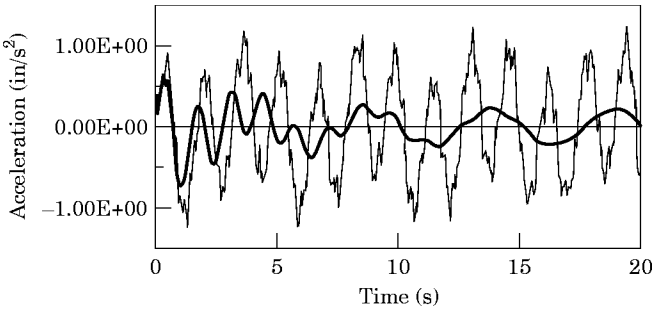

Figure 15. Comparison of the transverse acceleration response (low frequency harmonic loading, simply supported). Key as for Figure 3.

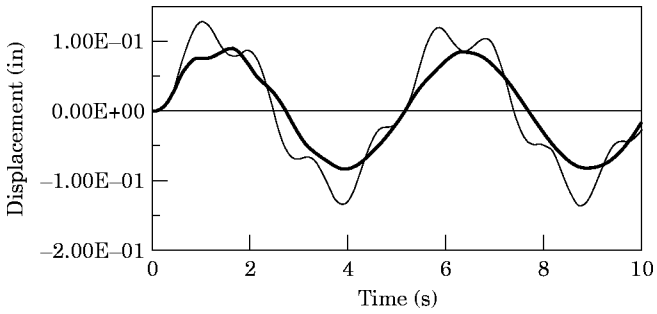

Figure 16. Comparison of the transverse displacement response (low frequency harmonic loading, clamped boundary condition). Key as for Figure 3.

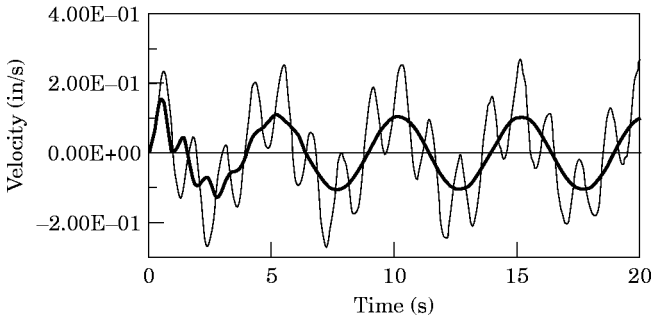

Figure 17. Comparison of the transverse velocity response (low frequency harmonic loading, clamped boundary condition). Key as for Figure 3.

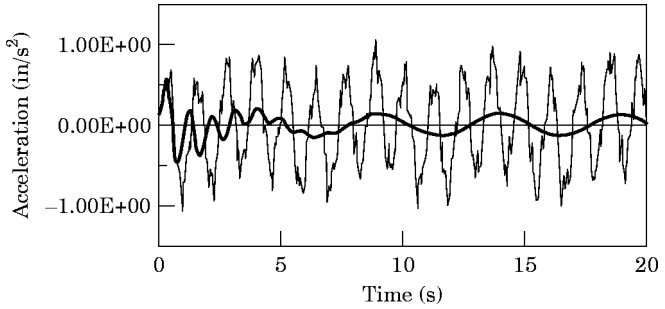

Figure 18. Comparison of the transverse acceleration response (low frequency harmonic loading, clamped boundary condition). Key as for Figure 3.

harmonic loading examples, a general reduction on the amplitudes of each response was obtained. This reduction appeared to be more effective on the acceleration responses for both of the simply supported and clamped beams. For the case without consideration of the viscoelastic behavior, the responses in the simply supported multilayer sandwich beam were generally larger than those in the beam with clamped boundary conditions during the low frequency harmonic loading. For the cases in which the viscoelastic behavior was taken into consideration, the displacement vibration was generally in accordance with the motion of loading, and the high frequency motions of the velocity and the acceleration were also transformed into a similar but flattening vibration motion during the later loading stage.

5.4. MULTILAYER SANDWICH BEAM SUBJECTED TO HIGH FREQUENCY HARMONIC LOADING

In this analysis, a loading at 2·0 Hz, relatively higher than the resonant frequency, was applied for both the simple beam and clamped beam system. Figures 19–21 show the comparison of the time domain response of the transverse displacement, velocity and acceleration respectively at the middle point of the multilayer sandwich beam with simply supported boundary condition. Figures 22 also shows the comparison of the response of the transverse displacement for the same beam but with a clamped boundary condition. In this analysis a general

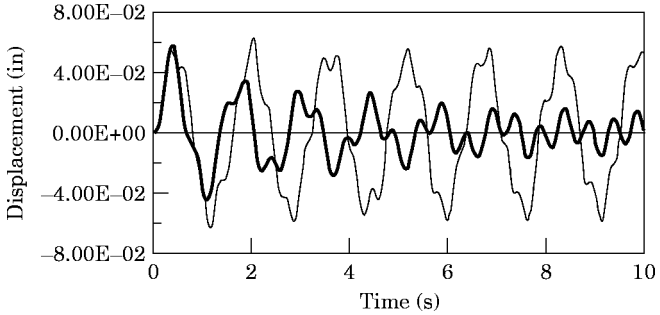

Figure 19. Comparison of the transverse displacement response (high frequency harmonic loading, simply supported). Key as for Figure 3.

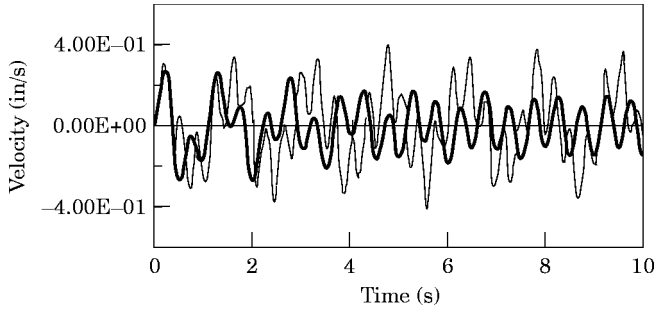

Figure 20. Comparison of the transverse velocity response (high frequency harmonic loading, simply supported). Key as for Figure 3.

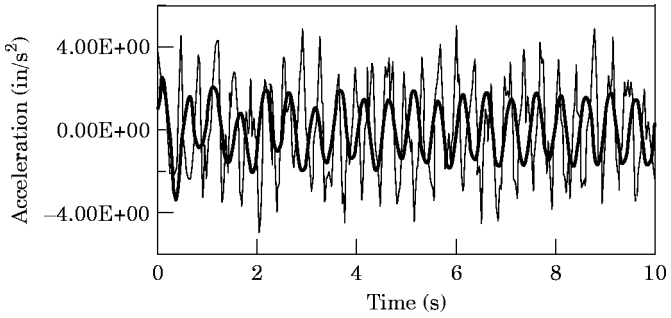

Figure 21. Comparison of the transverse acceleration response (high frequency harmonic loading, simply supported). Key as for Figure 3.

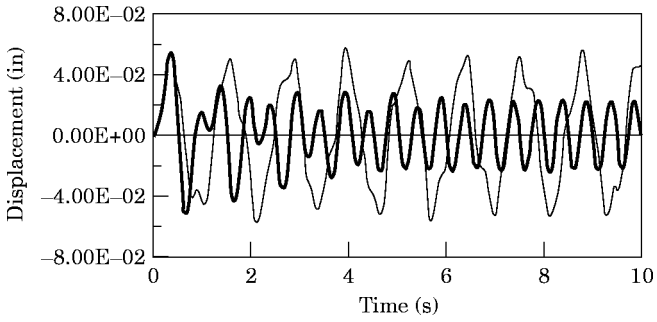

Figure 22. Comparison of the transverse displacement response (high frequency harmonic loading, clamped boundary condition). Key as for Figure 3.

reduction in the amplitudes of each response was obtained. For the cases in which the viscoelastic behavior was taken into consideration, the vibration motion of the velocity and the acceleration were generally in accordance with the loading motion and the displacement also adopted a similar motion during the later loading stage. Figure 23 presents a force–displacement relationship for the axial responses of a simply supported beam with consideration of viscoelastic behavior, where a typical mechanical behavior of viscoelastic material was observed.

5.5. MULTILAYER SANDWICH BEAM SUBJECTED TO RANDOM PROCESS

In the random loading analysis a broad band random process shown in Figure 24 was applied to the multilayer sandwich beam system with the clamped boundary condition. The random process with zero mean and spectral density $S_p(\omega)$ as shown in Figure 25, was obtained from the Monte Carlo technique [26], and expressed as a form of the sum of cosine functions:

$$P(t) = \sqrt{2} \sum_{j=1}^{N} A_j \cos(\omega_j t - \phi_j), \tag{31}$$

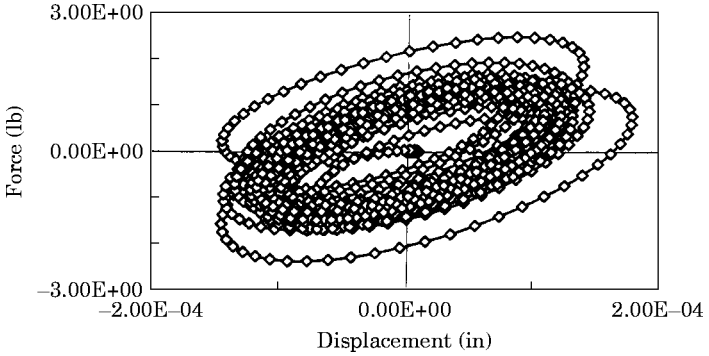

Figure 23. Force–displacement relationship for the axial responses (high frequency harmonic loading, simply supported).

where

$$A_j = \sqrt{2S_p(\omega_j)\Delta\omega}, \qquad \omega_j = (j - \tfrac{1}{2})\Delta\omega,$$

and ϕ_j are random angles uniformly distributed between 0 and 2π. It is noticed in Figure 25 that the broad band spectral density for the random process is in a frequency range between 0–20 Hz which covers the general frequencies of typical civil buildings. Figures 26 and 27 show a comparison of the response on the displacement and velocity respectively. Again, as indicated in the results a

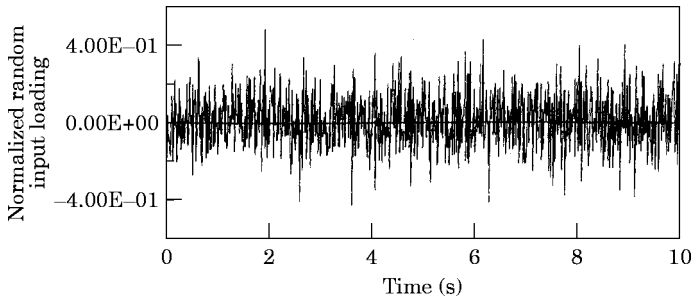

Figure 24. Normalized random process as loading input.

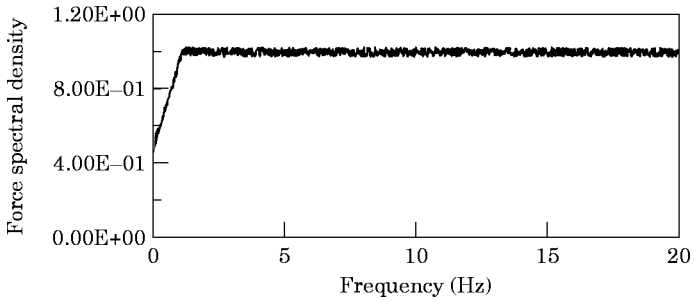

Figure 25. The broad band spectral density.

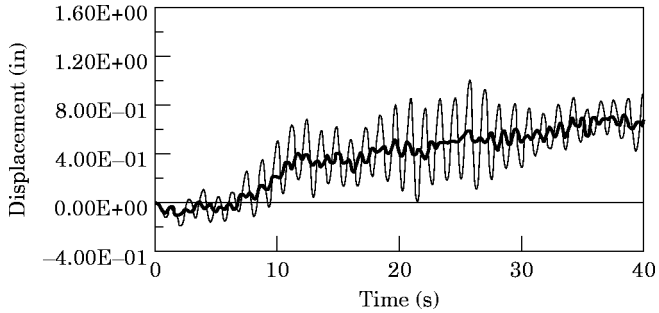

Figure 26. Comparison of the transverse displacement response (random loading, clamped boundary condition). Key as for Figure 3.

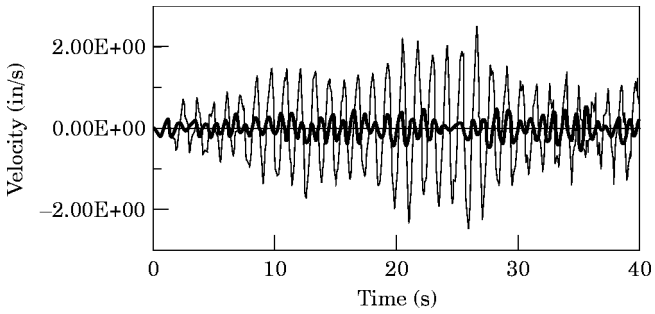

Figure 27. Comparison of the transverse velocity response (random loading, clamped boundary condition). Key as for Figure 3.

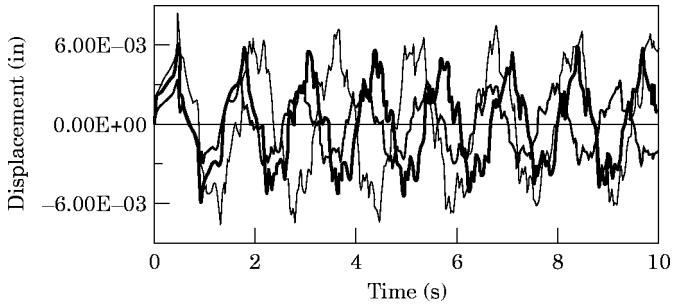

Figure 28. Comparison of the transverse displacement response (ignoring viscoelastic behavior, transient impulse, simply supported). Key: ——, original; ——, core layer doubled; ▬▬, stiff layers doubled.

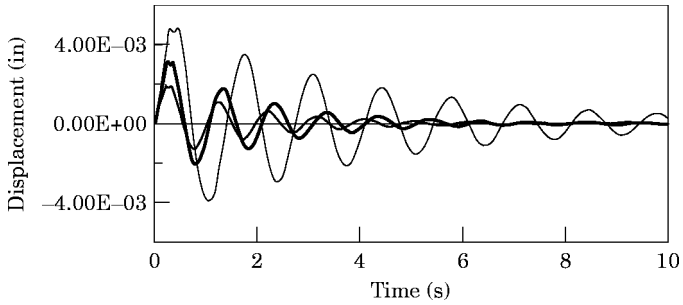

Figure 29. Comparison of the transverse displacement response (with viscoelastic behavior, transient impulse, simply supported). Key as for Figure 28.

reduction in both the displacement and velocity responses was observed when the viscoelastic material was incorporated into the beam system.

5.6. MULTILAYER SANDWICH BEAM WITH VARIANT THICKNESS ON THE STIFF AND CORE LAYERS

In this analysis, in order to observe the influence of dimensional factors on the dynamic behavior of the multilayer sandwich beam, the thickness of the stiff layers and the core layers were doubled alternately when subjected to a transient impulse, and the results were compared to the original beam as indicated in the first example. While the viscosity of the core was ignored, Figure 28 represents the

displacement responses when the thickness of the core and the stiff layers was increased respectively, compared to the displacement of the original sandwich beam. As illustrated in the figure, the amplitudes and the periods for the displacement response were both reduced due to the increase of the system stiffness. Figure 29 shows the same comparison of the displacement responses when the non-linear viscoelastic material behavior was taken into consideration. This figure also shows an initial reduction in the amplitude and period whereas a gradual decay in the amplitude with respect to the time was observed subsequently. By taking away the stiffness effect, for the beam with doubled thickness of the core layer, the initial amplitude drop due to the non-linear viscoelastic effect is about 53% compared to the beam with a similar stiffness but without viscosity. The damping factor estimated from the logarithmic decrement method is about 8·75% between two consecutive peaks. For the beam with doubled stiff layer thickness, the initial drop of the amplitude is about 54% and the damping factor is 8·70% between two consecutive peaks.

6. CONCLUDING REMARKS

As was shown in the analysis, the analytical method developed here could accurately describe the behavior of the viscoelastic material and provide a non-linear view in the time domain for the dynamic behavior of the multilayer sandwich beam system combined with the viscoelastic core layer. According to the numerical analytical analysis for the multilayer sandwich beam with viscoelastic core layer, no matter whether the loading is transient, resonant, harmonic or random type a general reduction in the responses of the displacement, velocity and acceleration was observed.

In the harmonic loading analysis during the low frequency input, the motion of the displacement was generally in accordance with the loading motion, and the motion of the velocity and acceleration was also transferred into a similar motion but with a phase difference and flattened amplitude in the latter loading stage. During the relatively high frequency input a similar phenomenon was observed: the response of the velocity and the acceleration was generally in accordance with the motion of loading while the displacement was transferred into a similar vibration motion only during the later loading stage. The reduction effect due to viscoelastic layers appears to be better for the acceleration response in the lower frequency loading case while the reduction effect is better for the displacement response when subjected to higher frequency loading.

The beam with clamped boundary condition, as expected, showed a stiffer mechanic behavior when the material characteristics of the viscoelastic core layers were ignored, but when the viscoelastic behavior of the core layers was counted, a similar dynamic behavior was found for both of the clamped beam and the simply supported beam. From the force–displacement relationship for the relative axial responses *of a simple supported beam with viscoelastic layer*, the typical mechanical behavior of viscoelastic material was observed.

In the dimensional effect analysis, when comparing the effects of thickness variation of the initial drop of the amplitude is about 10% higher for the beam

with doubled thickness of either stiff or core layers. The damping factor is about the same for the beam with doubled thickness of either the viscoelastic core-layer or the stiff-layer during the early loading stage, which is consistent with Kerwin's [2] observation for the sandwich beam at much higher frequencies. But the damping decayed during the later loading stage due to the non-linear deterioration characteristics of the material. However, the decaying phenomenon is insignificant when the thickness of either the viscoelastic core-layer or the stiff-layer is doubled.

REFERENCES

1. W. Swallow 1939 *British Patent Specification* 513171. An improved method of damping panel vibrations.
2. E. M. Kerwin Jr. 1959 *Journal of the Acoustical Society of America* **31**, 952–962. Damping of flexural waves by a constrained viscoelastic layer.
3. E. E. Ungar and E. M. Kerwin Jr. 1962 *Journal of the Acoustical Society of America* **34**, 954–957. Loss factors of viscoelastic systems in terms of energy concepts.
4. R. A. Di Taranto 1965 *Transactions of the ASME Journal of Applied Mechanics* **32**, 881–886. Theory of vibratory bending for elastic and viscoelastic layered finite-length beams.
5. R. A. Di Taranto and W. Blasingame 1966 *Journal of the Acoustical Society of America* **40**, 187–194. Composite loss factors of selected laminated beams.
6. R. A. Di Taranto and W. Blasingame 1967 *Transactions of the ASME Journal of Applied Mechanics*, 633–638. Composite damping of vibrating sandwich beams.
7. D. J. Mead and S. Markus 1969 *Journal of Sound and Vibration* **10**, 163–175. The forced vibration of three-layer, damped sandwich beam with arbitrary boundary conditions.
8. D. J. Mead 1982 *Journal of Sound and Vibration* **83**, 363–377. A comparison of some equations for the flexural vibration of a damped sandwich beam.
9. P. Mahmoodi 1972 *Journal of the Structural Division of ASCE* **95**, 1661–1667. Structural dampers.
10. D. M. Bergman and R. D. Hanson 1986 *Proceedings of the ATC Seminar and Workshop on Base Isolation and Passive Energy Dissipation*. *Applied Technology Council*, *Redwood City*, *CA*. Characteristics of viscoelastic damping devices.
11. R. C. Lin, Z. Liang and T. T. Soong 1988 *Technical Report NCEER*-88-0018, *State University at Buffalo*, *Buffalo*, *NY*. An experimental study of seismic structural response with added viscoelastic dampers.
12. K. C. Chang, T. T. Soong, S. T. Oh and M. L. Lai 1991 *Technical Report NCEER*-91-0012, *State University at Buffalo*, *Buffalo*, *NY*. Seismic response of a 2/5 scale steel structure with added viscoelastic dampers.
13. H. H. Lee and C.-S. Tsai 1992 *Proceedings of the* 10*th World Conference on Earthquake Engineering*, *Madrid Spain*. Analytical model for viscoelastic dampers in seismic mitigation application.
14. H. H. Lee and C.-S. Tsai 1994 *International Journal of Computers and Structures* **50**, 111–121. Analytical model of viscoelastic dampers for seismic mitigation of structures.
15. C.-S. Tsai and H. H. Lee 1992 *Proceedings of the ASCE Engineering Mechanics Conference*, *Texas A & M University*. Application of viscoelastic dampers to jointed structures for seismic mitigation.
16. C.-S. Tsai and H. H. Lee 1992 *PVP* **229**, *Doe Facilities Programs*, *System Interaction and Active/Inactive Damping ASME* (Edited by C.-W. Lin *et al*., pp. 113–118). Application of viscoelastic dampers to bridges for seismic mitigation.
17. C.-S. Tsai and H. H. Lee 1993 *Journal of Structural Engineering*, *ASCE* **119**, 1222–1233. Application of viscoelastic dampers to high-rise buildings.

18. C. S. Tsai and H. H. Lee 1993 *International Journal of Computers and Structures* **48**, 719–727. Seismic mitigation of bridges by using viscoelastic dampers.
19. R. H. Bagley and P. J. Torvik 1979 *Shock Vibration Bulletin* **49**, 135–143. A generalized derivative model for an elastomer damper.
20. R. H. Bagley 1983 *Journal of Rheology* **27**, 201–210. A theoretical basis for the application of fractional calculus to viscoelasticity.
21. B.-D. Liaw and R. W. Little 1967 *AIAA Journal* **5**, 301–304. Theory of bending multilayer sandwich plates.
22. J.-S. Kao and R. J. Ross 1968 *AIAA Journal* **6**, 1583–1585. Bending of multilayer sandwich beams.
23. T. P. Khatua and Y. K. Cheung 1973 *International Journal for Numerical Methods in Engineering* **6**, 11–24. Bending and vibration of multilayer sandwich beams and plates.
24. N. M. Newmark 1962 *Transactions of ASCE* **127**, 1406–1435. A method of computation for structural dynamics.
25. K. J. Bathe and E. L. Wilson 1976 *Numerical methods in finite element analysis*. Englewood Cliffs, NJ: Prentice-Hall.
20. S. O. Rice 1954 In: *Selected Papers on Noise and Stochastic Processes*, 180–181 (N. Wax, Editor). Dover, New York. Mathematical analysis of random noise.